Computers and Concrete, *Vol. 23, No. 4 (2019) 295-301*
DOI: https://doi.org/10.12989/cac.2019.23.4.295

Buckling analysis of concrete plates reinforced by piezoelectric nanoparticles

Reza Taherifar*[1], Maryam Mahmoudi[2], Mohammad Hossein Nasr Esfahani[3], Neda Ashrafi Khuzani[2], Shabnam Nasr Esfahani[4] and Farhad Chinaei[5]

[1]*Department of Civil Engineering, Meymeh Branch, Islamic Azad University, Meymeh, Iran*
[2]*Department of Computer Engineering, Meymeh Branch, Islamic Azad University, Meymeh, Iran*
[3]*Department of Mathematics, Faculty of Basic Science, Meymeh Branch, Islamic Azad University, Meymeh, Iran*
[4]*Department of Electrical Engineering, Meymeh Branch, Islamic Azad University, Meymeh, Iran*
[5]*Department of Civil and Mineral Engineering, Meymeh Branch, Islamic Azad University, Meymeh Iran*

(Received January 8, 2019, Revised March 28, 2019, Accepted April 5, 2019)

Abstract. In this paper, buckling analyses of composite concrete plate reinforced by piezoelectric nanoparticles is studied. The Halphin-Tsai model is used for obtaining the effective material properties of nano composite concrete plate. The nano composite concrete plate is modeled by Third order shear deformation theory (TSDT). The elastic medium is simulated by Winkler model. Employing nonlinear strains-displacements, stress-strain, the energy equations of concrete plate are obtained and using Hamilton's principal, the governing equations are derived. The governing equations are solved based on Navier method. The effect of piezoelectric nanoparticles volume percent, geometrical parameters of concrete plate and elastic foundation on the buckling load are investigated. Results showed that with increasing Piezoelectric nanoparticles volume percent, the buckling load increases.

Keywords: buckling; nanocomposite concrete plate; concrete plate; Reddy theory; Halphin-Tsai model

1. Introduction

Graphen concrete platelate has many applications in different industries due to the high hardness-to-weight and strength-to-weight ratios and other better properties compared with traditional isotropic ones. These structures can be used in aircraft, helicopters, missiles, launchers, satellites and etc. During the last 5 decades the application of sandwich structures with light core and two thin factsheets have been extensively investigated.

A new sinusoidal shear deformation theory was developed by Thai and Vo (2013) for bending, buckling, and vibration of functionally graded concrete plates. A simple refined shear deformation theory was proposed by Huu-Tai Thai *et al*. (2013) for bending, buckling, and vibration of thick concrete plates resting on elastic foundation. Forced vibration response of laminated composite and sandwich shell was studied by Kumar *et al*. (2014) using a 2D FE (finite element) model based on higher order zigzag theory (HOZT). Nonlocal dynamic buckling analysis of embedded micro concrete plates reinforced by single-walled carbon nano tubes was studied by Kolahchi and Cheraghbak (2017). Wang *et al*. (2018) investigated buckling of functionally graded Piezoelectric nanoparticles reinforced cylindrical shells consisting of multiple layers through FEM. Temperature-dependent buckling analysis of sandwich nano composite concrete plates resting on elastic medium subjected to magnetic field was studied by Shokravi (2017). Li *et al*. (2018) investigated the static linear elasticity, natural frequency, and buckling behaviour of functionally graded porous concrete plates reinforced by Piezoelectric nanoparticles. GPL-reinforced titanium (Ti) composites (GPL/Ti) were prepared by Liu *et al*. (2018) using spark plasma sintering to evaluate a new type of structural material. Gao *et al*. (2018) studied free vibration of functionally graded (FG) porous nano composite concrete plates reinforced with a small amount of Piezoelectric nanoparticles and supported by the two-parameter elastic foundations with different boundary conditions. Polit *et al*. (2018) investigated thick functionally graded graphene concrete platelets reinforced porous nano composite curved beams considering the static bending and elastic stability analyses based on a higher-order shear deformation theory accounting for through-thickness stretching effect. Transient dynamic analysis and elastic wave propagation in a functionally graded graphene concrete platelets (FGPiezoelectric nanoparticles)-reinforced composite thick hollow cylinder were presented by Hosseini and Zhang (2018). The in-plane and out-of-plane forced vibration of a curved nano composite micro beam were considered by Allahkarami *et al*. (2018). Transient heat transfer analysis of functionally graded (FG) carbon nano tube reinforced nano composite (CNTRC) cylinders with various essential and natural boundary conditions was investigated by Moradi-Dastjerdi and Payganeh (2018). Free vibration analyses of graphene reinforced singly and doubly curved laminated composite shell panels in thermal environment using finite element method were studied by Rout *et al*. (2019).

In this work, buckling analyses of composite concrete plate reinforced by piezoelectric nanoparticles is studied. The Halphin-Tsai model is used for obtaining the effective material properties of nano composite concrete plate. The

*Corresponding author, Research Engineer
E-mail: rtf_55@yahoo.com

ISSN: 1598-8198 (Print), 1598-818X (Online)

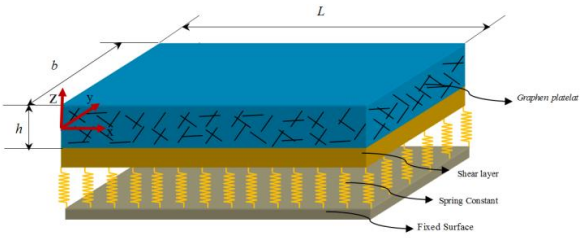

Fig. 1 A nanocomposite concrete plate reinforced by Piezoelectric nanoparticles resting on elastic medium

nano composite concrete plate is modeled by Third order shear deformation theory (TSDT). The elastic medium is simulated by Winkler model. Employing nonlinear strains-displacements, stress-strain, the energy equations of concrete plate are obtained and using Hamilton's principal, the governing equations are derived. The governing equations are solved based on Navier method. The effect of GPL volume percent, geometrical parameters of concrete plate and elastic foundation on the buckling load are investigated.

2. Kinematics of different theories

Fig. 1 shows a nanocomposite concrete plate reinforced by Piezoelectric nanoparticles resting on elastic medium.

Based on Third order shear deformation theory (TSDT), the orthogonal components of the displacement vector can be written as (Reddy 2002)

$$\begin{cases} u_1(x,y,z,t) = u(x,y,t) + z\,\phi_x(x,y,t) \\ +c_1 z^3\left(\phi_x + \dfrac{\partial w}{\partial x}\right), \\ u_2(x,y,z,t) = v(x,y,t) + z\,\phi_y(x,y,t) \\ +c_1 z^3\left(\phi_y + \dfrac{\partial w}{\partial y}\right), \\ u_3(x,y,z,t) = w(x,y,t), \end{cases} \tag{1}$$

However, the strain-displacement relations can be given as

$$\begin{pmatrix} \varepsilon_{xx} \\ \varepsilon_{yy} \\ \gamma_{xy} \end{pmatrix} = \begin{pmatrix} \varepsilon^0_{xx} \\ \varepsilon^0_{yy} \\ \gamma^0_{xy} \end{pmatrix} + z\begin{pmatrix} \varepsilon^1_{xx} \\ \varepsilon^1_{yy} \\ \gamma^1_{xy} \end{pmatrix} + z^3\begin{pmatrix} \varepsilon^3_{xx} \\ \varepsilon^3_{yy} \\ \gamma^3_{xy} \end{pmatrix}, \tag{2}$$

$$\begin{pmatrix} \gamma_{yz} \\ \gamma_{xz} \end{pmatrix} = \begin{pmatrix} \gamma^0_{yz} \\ \gamma^0_{xz} \end{pmatrix} + z^2\begin{pmatrix} \gamma^2_{yz} \\ \gamma^2_{xz} \end{pmatrix}, \tag{3}$$

where

$$\begin{pmatrix} \varepsilon^0_{xx} \\ \varepsilon^0_{yy} \\ \gamma^0_{xy} \end{pmatrix} = \begin{pmatrix} \dfrac{\partial u}{\partial x} \\ \dfrac{\partial v}{\partial y} \\ \dfrac{\partial u}{\partial y} + \dfrac{\partial v}{\partial x} \end{pmatrix}, \begin{pmatrix} \varepsilon^1_{xx} \\ \varepsilon^1_{yy} \\ \gamma^1_{xy} \end{pmatrix} = \begin{pmatrix} \dfrac{\partial \varphi_x}{\partial x} \\ \dfrac{\partial \varphi_y}{\partial y} \\ \dfrac{\partial \varphi_x}{\partial y} + \dfrac{\partial \varphi_y}{\partial x} \end{pmatrix},$$

$$\begin{pmatrix} \varepsilon^3_{xx} \\ \varepsilon^3_{yy} \\ \gamma^3_{xy} \end{pmatrix} = c_1\begin{pmatrix} \dfrac{\partial \varphi_x}{\partial x} + \dfrac{\partial^2 w}{\partial x^2} \\ \dfrac{\partial \varphi_y}{\partial y} + \dfrac{\partial^2 w}{\partial y^2} \\ \dfrac{\partial \varphi_x}{\partial y} + \dfrac{\partial \varphi_y}{\partial x} + 2\dfrac{\partial^2 w}{\partial x \partial y} \end{pmatrix}, \tag{4}$$

$$\begin{pmatrix} \gamma^0_{yz} \\ \gamma^0_{xz} \end{pmatrix} = \begin{pmatrix} \phi_y + \dfrac{\partial w}{\partial y} \\ \phi_x + \dfrac{\partial w}{\partial x} \end{pmatrix}, \begin{pmatrix} \gamma^2_{yz} \\ \gamma^2_{xz} \end{pmatrix} = c_2\begin{pmatrix} \phi_y + \dfrac{\partial w}{\partial y} \\ \phi_x + \dfrac{\partial w}{\partial x} \end{pmatrix}, \tag{5}$$

where $c_2=3c_1$.

Hence, the strain-stress of this theory can be written as

$$\begin{bmatrix} \sigma_{xx} \\ \sigma_{yy} \\ \sigma_{zz} \\ \sigma_{zy} \\ \sigma_{xz} \\ \sigma_{zy} \end{bmatrix} = \begin{bmatrix} C_{11} & C_{12} & C_{13} & 0 & 0 & 0 \\ C_{12} & C_{22} & C_{23} & 0 & 0 & 0 \\ C_{13} & C_{23} & C_{33} & 0 & 0 & 0 \\ 0 & 0 & 0 & C_{44} & 0 & 0 \\ 0 & 0 & 0 & 0 & C_{55} & 0 \\ 0 & 0 & 0 & 0 & 0 & C_{66} \end{bmatrix} \begin{bmatrix} \varepsilon_{xx} \\ \varepsilon_{yy} \\ \varepsilon_{zz} \\ \gamma_{zy} \\ \gamma_{xz} \\ \gamma_{xy} \end{bmatrix}, \tag{6}$$

where, parameters C_{ij} are elastic constant of composite concrete plate where can be obtained by Halpin-Tsai micro mechanics model. Based on this model, we have (Halpin and Kardos 1976)

$$E_c = \frac{3*(1+\xi_l V_{GPL})}{8*(1-\eta_L V_{GPL})} * E_m + \frac{5*(1+\xi_W \eta_W V_{GPL})}{8*(1-\eta_W V_{GPL})} * E_m \tag{7}$$

where

$$\eta_L = \frac{\left(\dfrac{E_{GPL}}{E_M}\right)-1}{\left(\dfrac{E_{GPL}}{E_M}\right)+\xi_L} \tag{8}$$

$$\eta_W = \frac{\left(\dfrac{E_{GPL}}{E_M}\right)-1}{\left(\dfrac{E_{GPL}}{E_M}\right)+\eta_L} \tag{9}$$

and E_c, E_m, E_{GPL} are the effective Young's moduli of the GPL/polymer nano composite, polymer matrix, and Piezoelectric nanoparticles, respectively. The effects of the geometry and size of GPL reinforcements are described through parameter.

$$\xi_L = 2\left(\frac{l_{GPL}}{h_{GPL}}\right); \tag{10}$$

$$\xi_W = 2\left(\frac{w_{GPL}}{h_{GPL}}\right) \tag{11}$$

in which l_{GPL}, w_{GPL} and h_{GPL} denote the length, width and thickness of the Piezoelectric nanoparticles. The volume fraction of Piezoelectric nanoparticles of the i-th layer can be obtained from GPL weight fraction fi and the mass densities of Piezoelectric nanoparticles and polymer matrix,

ρ_{GPL} and ρ_M, by

$$V_i = \frac{f_i}{f_i + \left(\frac{\rho_{GPL}}{\rho_M}\right)(1 - f_i)} \tag{12}$$

3. Motion equation

For driving the motion equations, the Hamilton principle is used as follows

$$\delta U - \delta W = 0 \tag{13}$$

where δ is variation, δU is variation of potential energy and δW is variation of external work.

The variation of potential energy for composite concrete plate can be written as

$$\mathrm{U} = \frac{1}{2}\int\begin{pmatrix}\sigma_{xx}\varepsilon_{xx} + \sigma_{yy}\varepsilon_{yy} + \sigma_{xy}\gamma_{xy} \\ +\sigma_{xz}\gamma_{xz} + \sigma_{yz}\gamma_{yz}\end{pmatrix}\mathrm{dV} \tag{14}$$

The variation of external work, due to elastic medium load simulated by Pasternak model can be express as

$$W_e = \int\int\left(-K_w w + K_g \nabla^2 w\right) w dA, \tag{15}$$

Using the Hamilton principle and partial integral, the governing equations are computed as

Equation 1:

$$\delta u : \frac{\partial N_{xx}}{\partial x} + \frac{\partial N_{xy}}{\partial y} = 0, \tag{16}$$

Equation 2:

$$\delta v : \frac{\partial N_{xy}}{\partial x} + \frac{\partial N_{yy}}{\partial y} = 0, \tag{17}$$

Equation 3:

$$\begin{aligned}&\delta w : \frac{\partial Q_{xx}}{\partial x} + \frac{\partial Q_{yy}}{\partial y} + c_2\left(\frac{\partial K_{xx}}{\partial x} + \frac{\partial K_{yy}}{\partial y}\right) + N_{xx}\frac{\partial^2 w}{\partial x^2} + N_{yy}\frac{\partial^2 w}{\partial y^2} \\ &-c_1\left(\frac{\partial^2 P_{xx}}{\partial x^2} + 2\frac{\partial^2 P_{xy}}{\partial x\,\partial y} + \frac{\partial^2 P_{yy}}{\partial y^2}\right) - K_w w + K_g \nabla^2 w = 0\end{aligned} \tag{18}$$

Equation 4:

$$\delta\phi_x : \frac{\partial M_{xx}}{\partial x} + \frac{\partial M_{xy}}{\partial y} + c_1\left(\frac{\partial P_{xx}}{\partial x} + \frac{\partial P_{xy}}{\partial y}\right) - Q_{xx} - c_2 K_{xx} = 0, \tag{19}$$

Equation 5:

$$\delta\phi_y : \frac{\partial M_{xy}}{\partial x} + \frac{\partial M_{yy}}{\partial y} + c_1\left(\frac{\partial P_{xy}}{\partial x} + \frac{\partial P_{yy}}{\partial y}\right) - Q_{yy} - c_2 K_{yy} = 0, \tag{20}$$

where, the force and moment resultants can be defined as:

$$\begin{Bmatrix}N_{xx} \\ N_{yy} \\ N_{xy}\end{Bmatrix} = \int_{-h/2}^{h/2}\begin{bmatrix}\sigma_{xx} \\ \sigma_{yy} \\ \sigma_{xy}\end{bmatrix} dz, \tag{21}$$

$$\begin{Bmatrix}M_{xx} \\ M_{yy} \\ M_{xy}\end{Bmatrix} = \int_{-h/2}^{h/2}\begin{bmatrix}\sigma_{xx} \\ \sigma_{yy} \\ \sigma_{xy}\end{bmatrix} z dz, \tag{22}$$

$$\begin{Bmatrix}P_{xx} \\ P_{yy} \\ P_{xy}\end{Bmatrix} = \int_{-h/2}^{h/2}\begin{bmatrix}\sigma_{xx} \\ \sigma_{yy} \\ \sigma_{xy}\end{bmatrix} z^3 dz, \tag{23}$$

$$\begin{bmatrix}Q_{xx} \\ Q_{yy}\end{bmatrix} = \int_{-h/2}^{h/2}\begin{bmatrix}\sigma_{xz} \\ \sigma_{yz}\end{bmatrix} dz, \tag{24}$$

$$\begin{bmatrix}K_{xx} \\ K_{yy}\end{bmatrix} = \int_{-h/2}^{h/2}\begin{bmatrix}\sigma_{xz} \\ \sigma_{yz}\end{bmatrix} z^2 dz, \tag{25}$$

$$I_i = \int_{-h/2}^{h/2}\rho z^i dz \qquad (i = 0,1,...,6), \tag{26}$$

$$J_i = I_i - \frac{4}{3h^2} I_{i+2} \qquad (i = 1,4), \tag{27}$$

$$K_2 = I_2 - \frac{8}{3h^2} I_4 + \left(\frac{4}{3h^2}\right)^2 I_6, \tag{28}$$

Therefore, the governing equations of nano composite concrete plate can be written as

$$\begin{aligned}&A_{11}\frac{\partial^2 u}{\partial x^2} + A_{12}\frac{\partial^2 v}{\partial x\,\partial y} + A_{16}\left(\frac{\partial^2 u}{\partial x\,\partial y} + \frac{\partial^2 v}{\partial x^2}\right) + B_{11}\frac{\partial^2 \varphi_x}{\partial x^2} \\ &+B_{12}\frac{\partial^2 \varphi_y}{\partial x\,\partial y} + B_{16}\left(\frac{\partial^2 \varphi_x}{\partial x\,\partial y} + \frac{\partial^2 \varphi_y}{\partial x^2}\right) + E_{11}c_1\left(\frac{\partial^2 \varphi_x}{\partial x^2} + \frac{\partial^3 w}{\partial x^3}\right) \\ &+E_{12}c_1\left(\frac{\partial^2 \varphi_y}{\partial x\,\partial y} + \frac{\partial^3 w}{\partial x\,\partial y^2}\right) + E_{16}c_1\left(\frac{\partial^2 \varphi_y}{\partial x^2} + \frac{\partial^2 \varphi_x}{\partial x\,\partial y} + 2\frac{\partial^3 w}{\partial x^2\partial y}\right) \\ &+A_{16}\frac{\partial^2 u}{\partial x\,\partial y} + A_{26}\frac{\partial^2 v}{\partial y^2} + A_{66}\left(\frac{\partial^2 u}{\partial y^2} + \frac{\partial^2 v}{\partial x\,\partial y}\right) + B_{16}\frac{\partial^2 \varphi_x}{\partial x\,\partial y} \\ &+B_{26}\frac{\partial^2 \varphi_y}{\partial y^2} + B_{66}\left(\frac{\partial^2 \varphi_x}{\partial y^2} + \frac{\partial^2 \varphi_y}{\partial x\,\partial y}\right) + E_{16}c_1\left(\frac{\partial^2 \varphi_x}{\partial x\,\partial y} + \frac{\partial^3 w}{\partial y\,\partial x^2}\right) \\ &+E_{26}c_1\left(\frac{\partial^2 \varphi_y}{\partial y^2} + \frac{\partial^3 w}{\partial y^3}\right) + E_{66}c_1\left(\frac{\partial^2 \varphi_y}{\partial x\,\partial y} + \frac{\partial^2 \varphi_x}{\partial y^2} + 2\frac{\partial^3 w}{\partial x\,\partial y^2}\right) = 0,\end{aligned} \tag{29}$$

$$\begin{aligned}&A_{16}\frac{\partial^2 u}{\partial x^2} + A_{26}\frac{\partial^2 v}{\partial x\,\partial y} + A_{66}\left(\frac{\partial^2 u}{\partial x\,\partial y} + \frac{\partial^2 v}{\partial x^2}\right) + B_{16}\frac{\partial^2 \varphi_x}{\partial x^2} \\ &+B_{26}\frac{\partial^2 \varphi_y}{\partial x\,\partial y} + B_{66}\left(\frac{\partial^2 \varphi_x}{\partial x\,\partial y} + \frac{\partial^2 \varphi_y}{\partial x^2}\right) + E_{16}c_1\left(\frac{\partial^2 \varphi_x}{\partial x^2} + \frac{\partial^3 w}{\partial x^3}\right) \\ &+E_{26}c_1\left(\frac{\partial^2 \varphi_y}{\partial x\,\partial y} + \frac{\partial^3 w}{\partial x\,\partial y^2}\right) + E_{66}c_1\left(\frac{\partial^2 \varphi_y}{\partial x^2} + \frac{\partial^2 \varphi_x}{\partial x\,\partial y} + 2\frac{\partial^3 w}{\partial x^2\partial y}\right) \\ &+A_{21}\frac{\partial^2 u}{\partial x\,\partial y} + A_{22}\frac{\partial^2 v}{\partial y^2} + A_{26}\left(\frac{\partial^2 u}{\partial y^2} + \frac{\partial^2 v}{\partial x\,\partial y}\right) + B_{21}\frac{\partial^2 \varphi_x}{\partial x\,\partial y} \\ &+B_{22}\frac{\partial^2 \varphi_y}{\partial y^2} + B_{26}\left(\frac{\partial^2 \varphi_x}{\partial y^2} + \frac{\partial^2 \varphi_y}{\partial x\,\partial y}\right) + E_{21}c_1\left(\frac{\partial^2 \varphi_x}{\partial x\,\partial y} + \frac{\partial^3 w}{\partial y\,\partial x^2}\right) \\ &+E_{22}c_1\left(\frac{\partial^2 \varphi_y}{\partial y^2} + \frac{\partial^3 w}{\partial y^3}\right) + E_{26}c_1\left(\frac{\partial^2 \varphi_y}{\partial x\,\partial y} + \frac{\partial^2 \varphi_x}{\partial y^2} + 2\frac{\partial^3 w}{\partial x\,\partial y^2}\right) = 0,\end{aligned} \tag{30}$$

$$
\begin{aligned}
&A_{55}\left(\frac{\partial^2 w}{\partial x^2}+\frac{\partial \varphi_x}{\partial x}\right)+A_{45}\left(\frac{\partial^2 w}{\partial x\,\partial y}+\frac{\partial \varphi_y}{\partial x}\right)+D_{55}c_2\left(\frac{\partial^2 w}{\partial x^2}+\frac{\partial \varphi_x}{\partial x}\right)\\
&+D_{45}c_2\left(\frac{\partial^2 w}{\partial x\,\partial y}+\frac{\partial \varphi_y}{\partial x}\right)+A_{45}\left(\frac{\partial^2 w}{\partial x\,\partial y}+\frac{\partial \varphi_x}{\partial y}\right)+A_{44}\left(\frac{\partial^2 w}{\partial y^2}+\frac{\partial \varphi_y}{\partial y}\right)\\
&+D_{45}c_2\left(\frac{\partial^2 w}{\partial x\,\partial y}+\frac{\partial \varphi_x}{\partial y}\right)+D_{44}c_2\left(\frac{\partial^2 w}{\partial y^2}+\frac{\partial \varphi_y}{\partial y}\right)\\
&+c_2\begin{pmatrix}D_{55}\left(\frac{\partial^2 w}{\partial x^2}+\frac{\partial \varphi_x}{\partial x}\right)+D_{45}\left(\frac{\partial^2 w}{\partial x\,\partial y}+\frac{\partial \varphi_y}{\partial x}\right)+F_{55}c_2\left(\frac{\partial^2 w}{\partial x^2}+\frac{\partial \varphi_x}{\partial x}\right)\\+F_{45}c_2\left(\frac{\partial^2 w}{\partial x\,\partial y}+\frac{\partial \varphi_y}{\partial x}\right)+D_{45}\left(\frac{\partial^2 w}{\partial x\,\partial y}+\frac{\partial \varphi_x}{\partial y}\right)+D_{44}\left(\frac{\partial^2 w}{\partial y^2}+\frac{\partial \varphi_y}{\partial y}\right)\\+F_{45}c_2\left(\frac{\partial^2 w}{\partial x\,\partial y}+\frac{\partial \varphi_x}{\partial y}\right)+F_{44}c_2\left(\frac{\partial^2 w}{\partial y^2}+\frac{\partial \varphi_y}{\partial y}\right)\end{pmatrix}\\
&+-K_w w+K_g\nabla^2 w-c_1\left(E_{11}\frac{\partial^3 u}{\partial x^3}+E_{12}\frac{\partial^3 v}{\partial x^2\partial y}+E_{16}\left(\frac{\partial^3 u}{\partial x^2\partial y}+\frac{\partial^3 v}{\partial x^3}\right)\right.\\
&+F_{11}\frac{\partial^3 \varphi_x}{\partial x^3}+F_{12}\frac{\partial^3 \varphi_y}{\partial x^2\partial y}+F_{16}\left(\frac{\partial^3 \varphi_x}{\partial x^2\partial y}+\frac{\partial^3 \varphi_y}{\partial x^3}\right)+H_{11}c_1\left(\frac{\partial^3 \varphi_x}{\partial x^3}+\frac{\partial^4 w}{\partial x^4}\right)\\
&+H_{12}c_1\left(\frac{\partial^3 \varphi_y}{\partial x^2\partial y}+\frac{\partial^4 w}{\partial x^2\partial y^2}\right)+H_{16}c_1\left(\frac{\partial^3 \varphi_y}{\partial x^3}+\frac{\partial^3 \varphi_x}{\partial x^2\partial y}+2\frac{\partial^4 w}{\partial x^3\partial y}\right)\\
&+E_{12}\frac{\partial^3 u}{\partial y^2\partial x}+E_{22}\frac{\partial^3 v}{\partial y^3}+E_{26}\left(\frac{\partial^3 u}{\partial y^3}+\frac{\partial^3 v}{\partial x\,\partial y^2}\right)\\
&+F_{12}\frac{\partial^3 \varphi_x}{\partial x\,\partial y^2}+F_{22}\frac{\partial^3 \varphi_y}{\partial y^3}+F_{26}\left(\frac{\partial^3 \varphi_x}{\partial y^3}+\frac{\partial^3 \varphi_y}{\partial x\,\partial y^2}\right)\\
&+H_{12}c_1\left(\frac{\partial^3 \varphi_x}{\partial x\,\partial y^2}+\frac{\partial^4 w}{\partial x^2\partial y^2}\right)+H_{22}c_1\left(\frac{\partial^3 \varphi_y}{\partial y^3}+\frac{\partial^4 w}{\partial y^4}\right)\\
&+H_{26}c_1\left(\frac{\partial^3 \varphi_y}{\partial x\,\partial y^2}+\frac{\partial^3 \varphi_x}{\partial y^3}+2\frac{\partial^4 w}{\partial x\,\partial y^3}\right)+2E_{16}\frac{\partial^3 u}{\partial y\,\partial x^2}+2E_{26}\frac{\partial^3 v}{\partial y^2\partial x}\\
&+2E_{66}\left(\frac{\partial^3 u}{\partial y^2\partial x}+\frac{\partial^3 v}{\partial x^2\partial y}\right)+2F_{16}\frac{\partial^3 \varphi_x}{\partial x^2\partial y}+2F_{26}\frac{\partial^3 \varphi_y}{\partial y^2\partial x}\\
&+2F_{66}\left(\frac{\partial^3 \varphi_x}{\partial y^2\partial x}+\frac{\partial^3 \varphi_y}{\partial x^2\partial y}\right)+2H_{16}c_1\left(\frac{\partial^3 \varphi_x}{\partial x^2\partial y}+\frac{\partial^4 w}{\partial x^3\partial y}\right)\\
&+2H_{26}c_1\left(\frac{\partial^3 \varphi_y}{\partial x\,\partial y^2}+\frac{\partial^4 w}{\partial y^3\partial x}\right)+2H_{66}c_1\left(\frac{\partial^3 \varphi_y}{\partial x^2\partial y}+\frac{\partial^3 \varphi_x}{\partial y^2\partial x}+2\frac{\partial^4 w}{\partial x^2\partial y^2}\right)\\
&+N_{xx}\frac{\partial^2 w}{\partial x^2}+N_{yy}\frac{\partial^2 w}{\partial y^2}=0,
\end{aligned}
\tag{31}
$$

$$
\begin{aligned}
&B_{11}\frac{\partial^2 u}{\partial x^2}+B_{12}\frac{\partial^2 v}{\partial x\,\partial y}+B_{16}\left(\frac{\partial^2 u}{\partial x\,\partial y}+\frac{\partial^2 v}{\partial x^2}\right)+D_{11}\frac{\partial^2 \varphi_x}{\partial x^2}\\
&+D_{12}\frac{\partial^2 \varphi_y}{\partial x\,\partial y}+D_{16}\left(\frac{\partial^2 \varphi_x}{\partial x\,\partial y}+\frac{\partial^2 \varphi_y}{\partial x^2}\right)+F_{11}c_1\left(\frac{\partial^2 \varphi_x}{\partial x^2}+\frac{\partial^3 w}{\partial x^3}\right)\\
&+F_{12}c_1\left(\frac{\partial^2 \varphi_y}{\partial x\,\partial y}+\frac{\partial^3 w}{\partial x\,\partial y^2}\right)+F_{16}c_1\left(\frac{\partial^2 \varphi_y}{\partial x^2}+\frac{\partial^2 \varphi_x}{\partial x\,\partial y}+2\frac{\partial^3 w}{\partial x^2\partial y}\right)\\
&+B_{16}\frac{\partial^2 u}{\partial x\,\partial y}+B_{26}\frac{\partial^2 v}{\partial y^2}+B_{66}\left(\frac{\partial^2 u}{\partial y^2}+\frac{\partial^2 v}{\partial x\,\partial y}\right)+D_{16}\frac{\partial^2 \varphi_x}{\partial x\,\partial y}\\
&+D_{26}\frac{\partial^2 \varphi_y}{\partial y^2}+D_{66}\left(\frac{\partial^2 \varphi_x}{\partial y^2}+\frac{\partial^2 \varphi_y}{\partial x\,\partial y}\right)+F_{16}c_1\left(\frac{\partial^2 \varphi_x}{\partial x\,\partial y}+\frac{\partial^3 w}{\partial y\,\partial x^2}\right)\\
&+F_{26}c_1\left(\frac{\partial^2 \varphi_y}{\partial y^2}+\frac{\partial^3 w}{\partial y^3}\right)+F_{66}c_1\left(\frac{\partial^2 \varphi_x}{\partial x\,\partial y}+\frac{\partial^2 \varphi_y}{\partial y^2}+2\frac{\partial^3 w}{\partial x\,\partial y^2}\right)\\
&+c_1\left(E_{11}\frac{\partial^2 u}{\partial x^2}+E_{12}\frac{\partial^2 v}{\partial x\,\partial y}+E_{16}\left(\frac{\partial^2 u}{\partial x\,\partial y}+\frac{\partial^2 v}{\partial x^2}\right)\right.\\
&+F_{11}\frac{\partial^2 \varphi_x}{\partial x^2}+F_{12}\frac{\partial^2 \varphi_y}{\partial x\,\partial y}+F_{16}\left(\frac{\partial^2 \varphi_x}{\partial x\,\partial y}+\frac{\partial^2 \varphi_y}{\partial x^2}\right)\\
&+H_{11}c_1\left(\frac{\partial^2 \varphi_x}{\partial x^2}+\frac{\partial^3 w}{\partial x^3}\right)+H_{12}c_1\left(\frac{\partial^2 \varphi_y}{\partial x\,\partial y}+\frac{\partial^3 w}{\partial x\,\partial y^2}\right)\\
&+H_{16}c_1\left(\frac{\partial^2 \varphi_y}{\partial x^2}+\frac{\partial^2 \varphi_x}{\partial x\,\partial y}+2\frac{\partial^3 w}{\partial x^2\partial y}\right)+E_{16}\frac{\partial^2 u}{\partial x\,\partial y}+E_{26}\frac{\partial^2 v}{\partial y^2}\\
&+E_{66}\left(\frac{\partial^2 u}{\partial y^2}+\frac{\partial^2 v}{\partial x\,\partial y}\right)+F_{16}\frac{\partial^2 \varphi_x}{\partial x\,\partial y}+F_{26}\frac{\partial^2 \varphi_y}{\partial y^2}+F_{66}\left(\frac{\partial^2 \varphi_x}{\partial y^2}+\frac{\partial^2 \varphi_y}{\partial x\,\partial y}\right)\\
&+H_{16}c_1\left(\frac{\partial^2 \varphi_x}{\partial x\,\partial y}+\frac{\partial^3 w}{\partial y\,\partial x^2}\right)+H_{26}c_1\left(\frac{\partial^2 \varphi_y}{\partial y^2}+\frac{\partial^3 w}{\partial y^3}\right)\\
&+H_{66}c_1\left(\frac{\partial^2 \varphi_y}{\partial x\,\partial y}+\frac{\partial^2 \varphi_x}{\partial y^2}+2\frac{\partial^3 w}{\partial x\,\partial y^2}\right)-A_{55}\left(\frac{\partial w}{\partial x}+\varphi_x\right)-A_{45}\left(\frac{\partial w}{\partial y}+\varphi_y\right)\\
&-D_{55}c_2\left(\varphi_x+\frac{\partial w}{\partial x}\right)-D_{45}c_2\left(\frac{\partial w}{\partial y}+\varphi_y\right)\\
&+c_2\begin{pmatrix}-D_{55}\left(\frac{\partial w}{\partial x}+\varphi_x\right)-D_{45}\left(\frac{\partial w}{\partial y}+\varphi_y\right)\\-F_{55}c_2\left(\varphi_x+\frac{\partial w}{\partial x}\right)-F_{45}c_2\left(\frac{\partial w}{\partial y}+\varphi_y\right)\end{pmatrix}=0,
\end{aligned}
\tag{32}
$$

$$
\begin{aligned}
&B_{16}\frac{\partial^2 u}{\partial x^2}+B_{26}\frac{\partial^2 v}{\partial x\,\partial y}+B_{66}\left(\frac{\partial^2 u}{\partial x\,\partial y}+\frac{\partial^2 v}{\partial x^2}\right)+D_{16}\frac{\partial^2 \varphi_x}{\partial x^2}\\
&+D_{26}\frac{\partial^2 \varphi_y}{\partial x\,\partial y}+D_{66}\left(\frac{\partial^2 \varphi_x}{\partial x\,\partial y}+\frac{\partial^2 \varphi_y}{\partial x^2}\right)+F_{16}c_1\left(\frac{\partial^2 \varphi_x}{\partial x^2}+\frac{\partial^3 w}{\partial x^3}\right)\\
&+F_{26}c_1\left(\frac{\partial^2 \varphi_y}{\partial x\,\partial y}+\frac{\partial^3 w}{\partial x\,\partial y^2}\right)+F_{66}c_1\left(\frac{\partial^2 \varphi_y}{\partial x^2}+\frac{\partial^2 \varphi_x}{\partial x\,\partial y}+2\frac{\partial^3 w}{\partial x^2\partial y}\right)\\
&+B_{12}\frac{\partial^2 u}{\partial x\,\partial y}+B_{22}\frac{\partial^2 v}{\partial y^2}+B_{26}\left(\frac{\partial^2 u}{\partial y^2}+\frac{\partial^2 v}{\partial x\,\partial y}\right)+D_{12}\frac{\partial^2 \varphi_x}{\partial x\,\partial y}\\
&+D_{22}\frac{\partial^2 \varphi_y}{\partial y^2}+D_{26}\left(\frac{\partial^2 \varphi_x}{\partial y^2}+\frac{\partial^2 \varphi_y}{\partial x\,\partial y}\right)+F_{12}c_1\left(\frac{\partial^2 \varphi_x}{\partial x\,\partial y}+\frac{\partial^3 w}{\partial y\,\partial x^2}\right)\\
&+F_{22}c_1\left(\frac{\partial^2 \varphi_y}{\partial y^2}+\frac{\partial^3 w}{\partial y^3}\right)+F_{26}c_1\left(\frac{\partial^2 \varphi_y}{\partial x\,\partial y}+\frac{\partial^2 \varphi_x}{\partial y^2}+2\frac{\partial^3 w}{\partial x\,\partial y^2}\right)\\
&+c_1\left(E_{16}\frac{\partial^2 u}{\partial x^2}+E_{26}\frac{\partial^2 v}{\partial x\,\partial y}+E_{66}\left(\frac{\partial^2 u}{\partial x\,\partial y}+\frac{\partial^2 v}{\partial x^2}\right)\right.\\
&+F_{16}\frac{\partial^2 \varphi_x}{\partial x^2}+F_{26}\frac{\partial^2 \varphi_y}{\partial x\,\partial y}+F_{66}\left(\frac{\partial^2 \varphi_x}{\partial x\,\partial y}+\frac{\partial^2 \varphi_y}{\partial x^2}\right)+H_{16}c_1\left(\frac{\partial^2 \varphi_x}{\partial x^2}+\frac{\partial^3 w}{\partial x^3}\right)\\
&+H_{26}c_1\left(\frac{\partial^2 \varphi_y}{\partial x\,\partial y}+\frac{\partial^3 w}{\partial x\,\partial y^2}\right)+H_{66}c_1\left(\frac{\partial^2 \varphi_y}{\partial x^2}+\frac{\partial^2 \varphi_x}{\partial x\,\partial y}+2\frac{\partial^3 w}{\partial x^2\partial y}\right)\\
&+E_{12}\frac{\partial^2 u}{\partial x\,\partial y}+E_{22}\frac{\partial^2 v}{\partial y^2}+E_{26}\left(\frac{\partial^2 u}{\partial y^2}+\frac{\partial^2 v}{\partial x\,\partial y}\right)+F_{12}\frac{\partial^2 \varphi_x}{\partial x\,\partial y}+F_{22}\frac{\partial^2 \varphi_y}{\partial y^2}\\
&+F_{26}\left(\frac{\partial^2 \varphi_x}{\partial y^2}+\frac{\partial^2 \varphi_y}{\partial x\,\partial y}\right)+H_{12}c_1\left(\frac{\partial^2 \varphi_x}{\partial x\,\partial y}+\frac{\partial^3 w}{\partial y\,\partial x^2}\right)+H_{22}c_1\left(\frac{\partial^2 \varphi_y}{\partial y^2}+\frac{\partial^3 w}{\partial y^3}\right)\\
&+H_{26}c_1\left(\frac{\partial^2 \varphi_y}{\partial x\,\partial y}+\frac{\partial^2 \varphi_x}{\partial y^2}+2\frac{\partial^3 w}{\partial x\,\partial y^2}\right)-A_{45}\left(\frac{\partial w}{\partial x}+\varphi_x\right)-A_{44}\left(\frac{\partial w}{\partial y}+\varphi_y\right)\\
&-D_{45}c_2\left(\varphi_x+\frac{\partial w}{\partial x}\right)-D_{44}c_2\left(\frac{\partial w}{\partial y}+\varphi_y\right)\\
&+c_2\begin{pmatrix}-D_{45}\left(\frac{\partial w}{\partial x}+\varphi_x\right)-D_{44}\left(\frac{\partial w}{\partial y}+\varphi_y\right)\\-F_{45}c_2\left(\varphi_x+\frac{\partial w}{\partial x}\right)-F_{44}c_2\left(\frac{\partial w}{\partial y}+\varphi_y\right)\end{pmatrix}=0,
\end{aligned}
\tag{33}
$$

where

$$A_{ij}=\int_{-h/2}^{h/2}Q_{ij}dz\,,\qquad (i,j=1,2,6) \tag{34}$$

$$B_{ij}=\int_{-h/2}^{h/2}Q_{ij}z\,dz\,, \tag{35}$$

$$D_{ij}=\int_{-h/2}^{h/2}Q_{ij}z^2dz\,, \tag{36}$$

$$E_{ij}=\int_{-h/2}^{h/2}Q_{ij}z^3dz\,, \tag{37}$$

$$F_{ij}=\int_{-h/2}^{h/2}Q_{ij}z^4dz\,, \tag{38}$$

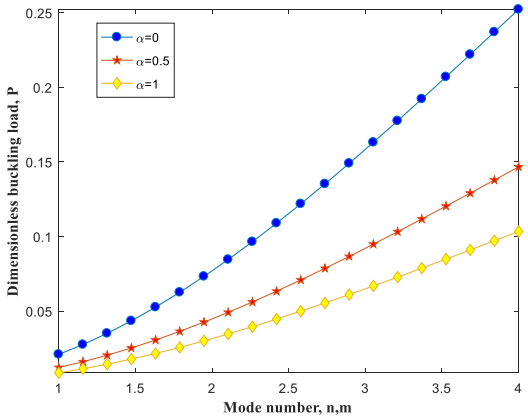

Fig. 2 Dimensionless buckling load versus mode number for different transverse to axial lode ratio

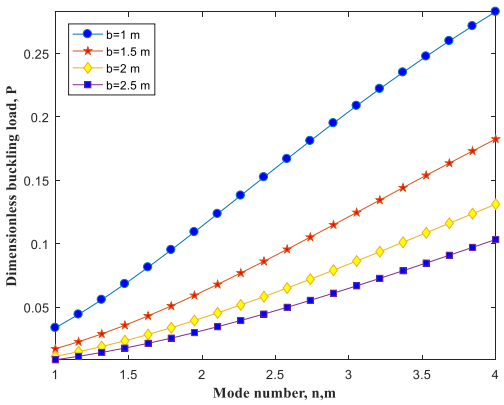

Fig. 3 The effect of concrete plate width on the dimensionless buckling load versus mode number

$$H_{ij} = \int_{-h/2}^{h/2} Q_{ij} z^6 dz, \tag{39}$$

4. Solution method

Base on Navier method, the displacements of the composite concrete plate with simply supported boundary condition can be written as

$$u(x,y,t) = u_0 \cos(\frac{n\pi x}{L}) \sin(\frac{m\pi y}{b}) e^{i\omega t}, \tag{40}$$

$$v(x,y,t) = v_0 \sin(\frac{n\pi x}{L}) \cos(\frac{m\pi y}{b}) e^{i\omega t}, \tag{41}$$

$$w(x,y,t) = w_0 \sin(\frac{n\pi x}{L}) \sin(\frac{m\pi y}{b}) e^{i\omega t}, \tag{42}$$

$$\phi_x(x,y,t) = \psi_{x0} \cos(\frac{n\pi x}{L}) \sin(\frac{m\pi y}{b}) e^{i\omega t}, \tag{43}$$

$$\phi_y(x,y,t) = \psi_{y0} \sin(\frac{n\pi x}{L}) \cos(\frac{m\pi y}{b}) e^{i\omega t}, \tag{44}$$

where, n is vibration mode number and ω is frequency. Substituting Eqs. (40)-(44) into Eqs. (29)-(33), the motion equations in matrix form can be expressed as

$$[K] \begin{bmatrix} u_0 \\ v_0 \\ w_0 \\ \psi_{x0} \\ \psi_{y0} \end{bmatrix} = 0, \tag{45}$$

where $[k_{ij}]$ is stiffness matrix.

5. Numerical result and discussion

In this section, a parametric study is done for the effects of different parameters on the nonlinear buckling load of the composite structure.

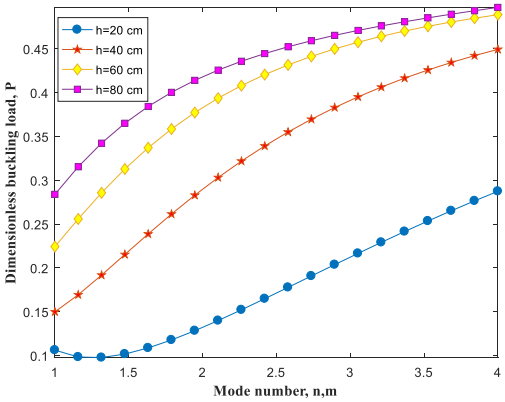

Fig. 4 The effect concrete plate thickens on the dimensionless buckling load versus mode number

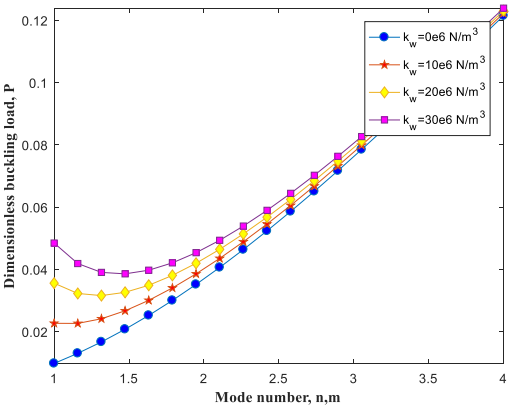

Fig. 5 The effect of spring constant of elastic medium on the dimensionless buckling load versus mode number

Figs. 2 and 3 show the effect of different transverse to axial lode ratio and concrete plate width on the buckling load versus mode number, respectively. As it is inferred with increasing transverse to axial lode ratio and concrete plate width, the buckling load has reduction. It is because with increasing transverse to axial lode ratio and concrete plate width, stiffness of system is decreased. In addition, increasing mode number, buckling load is increased.

Fig. 4 illustrates the effect of concrete plate thickness on the buckling lode versus mode number. It can be concluded

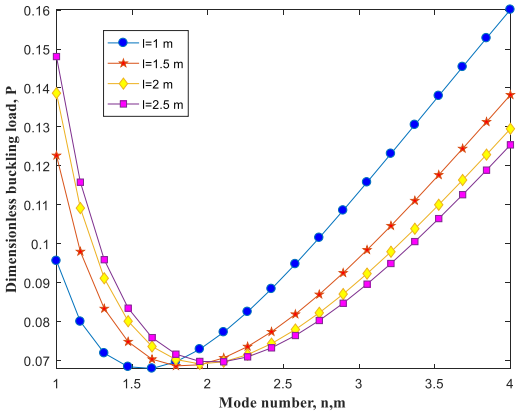

Fig. 6 The effect of concrete plate length on the dimensionless buckling load versus mode number

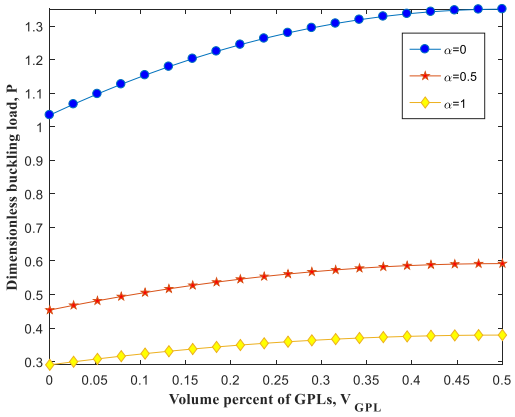

Fig. 7 Dimensionless buckling load versus volume percent of Piezoelectric nanoparticles for different transverse to axial lode ratio

with concrete plate thickness increases, stiffness of system is increased. It is because the buckling load is increased.

Fig. 5 indicates the effect of spring constant of elastic medium on the buckling load with respect to mode number. It is observed that with increasing spring constant of elastic medium, the buckling load is increased. It is because stiffness of system is increased with enhancing spring constant of elastic medium.

The effect of concrete plate length on the buckling load as function of mode number is shown in Fig. 6. With increasing concrete plate length, buckling load decreases. It is because stiffness of structure is decreased.

Fig. 7 shows buckling load versus volume present of GPL for different transverse to axial lode ratio. As can be seen, the buckling load of micro composite structure with increasing transverse to axial lode ratio is decreased. Furthermore, with increasing the GPL volume percent, the buckling load is increased due to increase in the bending rigidity of the structure.

The effect of volume percent of Piezoelectric nanoparticles on the buckling load is shown in Fig. 8 for different length to thickness ratio of the Piezoelectric nanoparticles (zeta). It is found that with increasing the zeta, the buckling load is decreased due to the enhance in the stiffness of the structure.

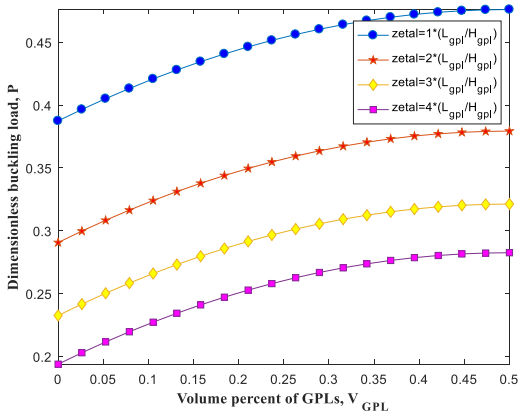

Fig. 8 The effect of volume percent of Piezoelectric nanoparticles on the dimensionless buckling load for different length to thickness ratio of the Piezoelectric nanoparticles

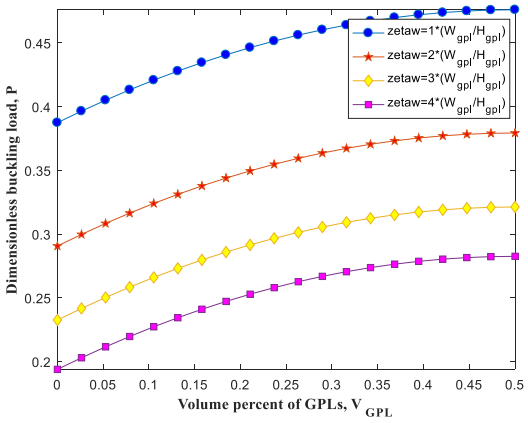

Fig. 9 The effect of weight to thickness ratio of Piezoelectric nanoparticles on the buckling load versus volume percent of Piezoelectric nanoparticles

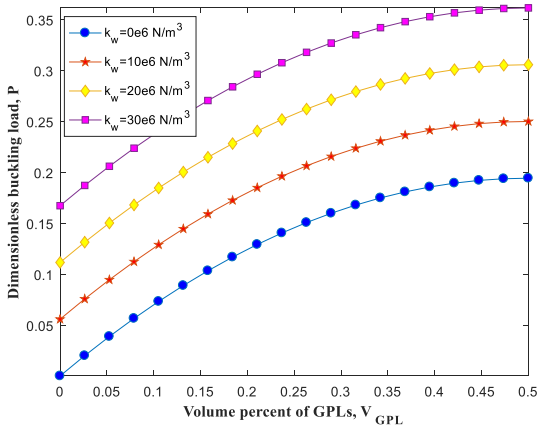

Fig. 10 The effect of spring constant of elastic medium on the buckling load versus volume percent of Piezoelectric nanoparticles

Fig. 9 shows the effect of weight to thickness ratio of Piezoelectric nanoparticles (zetaw) on the buckling load versus volume percent of Piezoelectric nanoparticles. As can be seen, with increasing zetaw, the buckling load is decreased. It is since with increasing zetaw, the stiffness is

decreased.

Fig. 10 indicates the effect of spring constant of elastic medium on the buckling load with respect to volume percent of Piezoelectric nanoparticles. It is observed that with increasing spring constant of elastic medium, the buckling load is increased. It is because stiffness of system is increased with enhancing spring constant of elastic medium

5. Conclusions

In this work, buckling analyses of composite concrete plate reinforced by GPL restiong on elastic medium was presented. The elastic medium was simulated by Winkler model. The Halpin-Tsai model for considering effect of Piezoelectric nanoparticles was used. The motion equations were calculated by TSDT, Hamilton's principle and energy method. Using analytical method, the buckling load of the structure was obtained. The effect of GPL volume percent, geometrical parameters of concrete plate and elastic foundation on the buckling load were investigated. Increasing volume percent of Piezoelectric nanoparticles, buckling load was increased. Increasing spring constant of elastic medium, the buckling load was increased. In addition, with increasing zeta, buckling lode decreases.

Reference

Allahkarami, F., Nikkhah-bahrami, M. and Ghassabzadeh Saryazdi, M. (2018), "Nonlinear forced vibration of FG-CNTs-reinforced curved microbeam based on strain gradient theory considering out-of-plane motion", *Steel Compos. Struct*, **22**, 673-691.

Gao, K., Gao, W., Chen, D. and Yang, J. (2018), "Nonlinear free vibration of functionally graded graphene concrete platelets reinforced porous nano composite concrete plates resting on elastic foundation", *Compos. Struct*., **204**, 831-846.

Halpin, J.C. and Kardos, J.L. (1976), "The Halpin-Tsai equations: a review", *Polym. Eng. Sci*., **16**(5), 344-352.

Hosseini, S.M. and Zhang, Ch. (2018), "Elastodynamic and wave propagation analysis in a FG Graphene concrete platelets-reinforced nanocomposite cylinder using a modified nonlinear micromechanical model", *Steel Compos. Struct*., **27**, 255-271.

Kolahchi, R. and Cheraghbak, A. (2017), "Agglomeration effects on the dynamic buckling of visco elastic micro concrete plates reinforced with SWCNTs using Bolotin method", *Nonlin. Dyn*., **90**, 479-492

Kumar, A., Chakrabarti, A. and Bhargava, P. (2014), "Accurate dynamic response of laminated composites and sandwich shells using higher order zigzag theory", *Thin Wall. Struct*., **77**, 174-186.

Li, K., Wu, D., Chen X., Cheng J., Liu Zh., Gao, W. and M. Liu, (2018), "Isogeometric analysis of functionally graded porous concrete plates reinforced by graphene concrete platelets", *Compos. Struct*., **204**, 114-130.

Liu, J., Wu, M., Yang, Y., Yang, G., Yan, H. and Jiang, K. (2018), "Preparation and mechanical performance of graphene concrete platelet reinforced titanium nanocomposites for high temperature applications", *Comput. Concrete*, **22**, 355-363.

Polit, O., Anant, C., Anirudh, B. and Ganapathi, M. (2019), "Functionally graded graphene reinforced porous nanocomposite curved beams: Bending and elastic stability using a higher-order model with thickness stretch effect", *Compos. Part B: Eng*., **166**, 310-327.

Reddy, J.N. (2002), *Mechanics of Laminated Composite Concrete Plates and Shells: Theory and Analysis*, Second Edition, CRC Press.

Rout, M., Hot, S.S. and Karmakar, A. (2019), "Thermoelastic free vibration response of graphene reinforced laminated composite shells", *Eng. Struct.*, **178**, 179-190

Shokravi, M. (2017), "Buckling of sandwich concrete plates with FG-CNT-reinforced layers resting on orthotropic elastic medium using Reddy concrete plate theory", *Steel Compos. Struct*., **23**, 623-631.

Thai, H. and Vo, T. (2013), "A new sinusoidal shear deformation theory for bending, buckling and vibration of functionally graded concrete plates", *Appl. Math. Model*., **37**, 3269-3281.

Thai, H., Park, M. and Choi, D. (2013), "A simple refined theory for bending, buckling, and vibration of thick concrete plates resting on elastic foundation", *Int. J. Mech. Sci*., **73**, 40-52.

Wang, Y., Feng, Ch., Zhao, Zh. and Yang, J. (2018), "Eigenvalue buckling of functionally graded cylindrical shells reinforced with graphene concrete platelets (GPL)", *Compos. Struct*., **20**, 238-246.

CC